

# Dilepton/photon production in heavy ion collisions, and the QCD phase transition

C.M. Hung<sup>1</sup> and E.V. Shuryak<sup>2</sup>

Department of Physics  
State University of New York at Stony Brook  
Stony Brook, New York 11794

## Abstract

We calculate electromagnetic production from highly excited hadronic matter created in heavy ion collisions. The rates include the usual lowest order processes in quark-gluon plasma plus the usual reactions in the hadronic phase, related with  $\rho, a_1$  mesons. The space-time integration is done using a hydrodynamical model. We have found that dilepton mass spectrum agrees with results of other previous works, but *disagrees* with the CERES dilepton data. In order to explain these data, some “unconventional” production mechanism need to be incorporated: we discuss especially the notion of modified  $\rho, a_1$  masses, which indeed may explain the data. Other suggestions (e.g. the longer-lived fireball) to increase the production of low mass dileptons seem to be insufficient for the task. The results for direct photon production are below the current WA80 experimental bounds, for all variants considered.

---

<sup>1</sup>Email: cmhung@insti.physics.sunysb.edu

<sup>2</sup>Email: shuryak@dau.physics.sunysb.edu

# 1 Introduction

The main goal of heavy-ion collision program in the AGS/SPS energy range (10-200 GeV/A) is to produce hot/dense hadronic matter with the energy density of the order of few  $GeV/fm^3$  and to study its properties. Especially interesting are *early* stages of the collisions, when theory predicts existence of the QCD phase transition into a new phase, called the Quark-Gluon Plasma (QGP). However, so far no direct experimental evidence of the QGP has been found. The main reason for this is well known: strong collective interaction in the system as it expands and cools erases most of the traces of the dense stage. As a result, the observed hadrons come mostly from a dilute freeze-out stage, with a *final* temperature  $T_f = 120 - 140 MeV$ . [1]

One possible way to study the earlier stages (to be discussed in this paper) is to look for phenomena which mostly happen very soon after the collision, such as production of *dileptons* and *photons*<sup>3</sup>[2]. At high (RHIC/LHC) energies one may hope for some kinematic enhancement of the QGP signals because the initial stage is much hotter than hadronic matter,  $T_i \gg T_c$  [3, 4], but this is certainly *not* the case for AGS/SPS energies. Therefore, in this energy domain the main signals for the phase transition still come from the *hadronic* stage, not the QGP.

Experiments designed to observe the *direct photons* or *dilepton continuum* produced by excited hadronic matter in heavy ion collisions are generally much more difficult to perform compared with measurements of hadronic observables. Therefore, only recently were the first photon and dilepton measurements announced by four CERN SPS experiments: NA34/3, NA38

---

<sup>3</sup>Another possibility is to look for signals which are *accumulated* during the evolution: the well known examples include excessive production of strangeness or charmonium suppression.

and CERES (NA45) for dileptons and WA80 for photons. It was found that dilepton production exceeds backgrounds expected from hadronic and charm decays. Furthermore, the signal also exceeds theoretical expectations for “conventional” processes, both in hadronic and quark-gluon matter [5]. Especially dramatic is the excess observed by CERES [6] in the mass region  $M_{e^+e^-} = 0.3 - 0.6$  GeV. This observation has since created a rapidly growing theoretical literature.

Calculation of the dilepton/photon yield consists of two components: (i) evaluation of production *rates* (see section 2); and (ii) their integration over the *space-time evolution* of the collision (see section 3). In the so called *conservative* approach (the well-known hadronic processes with vacuum parameters and the usual space-time evolution of heavy-ion collisions) several groups have obtained rather similar results, which however do not explain the CERES data, neither in magnitude nor even in the shape of the mass spectrum.

This situation has lead to many “unconventional” hypotheses, which include (in a more or less chronological order): (i) dropping  $m_\rho$  [8, 7]; (ii) high pion occupation numbers at low momenta [9]; (iii) a very long-lived fireball [5]; (iv) dropping  $m_{\eta'}$  [10, 11, 12]; (v) a modified pion dispersion curve [13]; (vi) dropping  $m_{a_1}$  (discussed below).

Let us start with the possibility (ii), which is usually taken into account by introduction of the pion chemical potential  $\mu_\pi$ , which is approximately equal to  $m_\pi$ . Although the true nature of the low- $p_t$  pions is not yet completely clear, most probably they come from the resonance decay and/or spectral modification due to collective potentials. Both are late-stage phenomena, which can hardly affect the early-stage dilepton production. Furthermore, studies of this explanation made in [7] have shown, that the low-M dilepton enhancement due to  $\mu_\pi \approx m_\pi$  is way too small compared to CERES data.

In section 5 we will look at (i), the T-dependent  $m_\rho$ , and (similar to [7]) conclude that it may indeed describe the data. Furthermore, we have linked it to (vi) by theoretical arguments related to chiral symmetry restoration and

have derived experimental consequences of the most plausible scenario, both for dilepton and photon (section 8 ) yields.

We also study separately a proposal (iii). In our previous paper [14], we found that (at least in a hydro approach) the so called “softest point” of the Equation of State (EOS) leads to especially long-lived fireball. Although it is expected to happen at collision energies way below those for CERN experiments, in section 7 we have pushed this idea to the extreme and assumed the scenario with the long-lived fireball. The results for the dileptons are quite disappointing: very different scenarios of space-time evolutions give very similar dilepton mass spectra. So, with the standard dilepton rates and fixed masses it is not possible to explain the observed dilepton yield by longer lifetime.

## 2 Electromagnetic processes in hadronic matter

Dilepton/photon production in the QGP phase is based on fundamental QCD processes like  $\bar{q}q \rightarrow e^+e^-$  [2] and was calculated long ago. The rate in the pion gas due to  $\pi\pi$  annihilation was considered in [15], and those two basic processes can be included by the “standard rate” formula:

$$\frac{dR}{d^4q} = \frac{\alpha^2}{48\pi^4} F e^{-\frac{q_0}{T}} \quad (1)$$

where the rate  $R$  is counted per unit volume per unit time,  $q$  is 4-momentum of the virtual photon ( $q^2 = M_{e^+e^-}^2 = M^2$ ),  $F$  is a constant in QGP and the usual pion form-factor in the pion gas, which can be written in standard

vector-dominance form <sup>4</sup>

$$F = \begin{cases} F_H \stackrel{\text{def}}{=} \frac{m_\rho^4}{[(m_\rho^2 - M^2)^2 + m_\rho^2 \Gamma_\rho^2]}, & \text{(Hadronic)} \\ F_Q \stackrel{\text{def}}{=} 12 \sum_q e_q^2 \left(1 + \frac{2m_q^2}{M^2}\right) \left(1 - \frac{4m_q^2}{M^2}\right)^{\frac{1}{2}}, & \text{(QGP)} \end{cases} \quad (2)$$

Later additional processes including  $\rho$  mesons were added. It was also pointed out in [16] that  $a_1$  meson is very important<sup>5</sup>, especially for photons and low-mass dileptons. Further work was done in refs. [17, 18].

Before we come to specific formulae, let us remark on some misunderstanding of the role of the resonances, which has even led to double counting in some previous papers. Unstable particles like  $\rho$  meson can be considered either (i) as parents of decay processes (such as  $\rho \rightarrow e^+e^-$ ,  $a_1 \rightarrow e^+e^-\pi$ ) or (ii) as intermediate states in particular reactions with “stable” particles (e.g.  $\pi^+\pi^- \rightarrow e^+e^-$ ). Furthermore, the same resonance can enter as an intermediate stage in many different reactions: This created the impression that by considering many of these reactions, one can in fact increase the dilepton yield.

However, this is not true. In *thermal equilibrium* the average number of mesons depends on their mass but should *not* depend on their width (which only shows how often these particles are created and decay). In order to understand how this happens (we’ll give detailed discussion in the Appendix), recall that standard Breit-Wigner amplitude is proportional to  $\Gamma_{in}\Gamma_{out}/((M - M_{res})^2 + \Gamma_{tot}^2/4)$ . Summing over all possible “in” channel one gets  $\Gamma_{tot}$  in the numerator, and after that one may approximately<sup>6</sup> substitute the Breit-Wigner amplitude simply by  $\Gamma_{out}\delta(M - M_{res})$ . The resulting rate is nothing

---

<sup>4</sup>For the quark masses, we adopt the perturbative result [15]  $m_q(T) = \frac{gT}{\sqrt{6}}$ , with  $g = 2.05$  which corresponds to  $\alpha_s = 0.33$ .

<sup>5</sup> In order to explain why  $a_1$  is important, let us go “backward in time”: it is the first hadronic resonance which may be excited in a collision of a photon, real or virtual, with a pion.

<sup>6</sup>Provided the total width is not large compared with the temperature!

else but the decay contribution (i) mentioned above: clearly one should not include it twice. We have found it rather convenient for our applications to

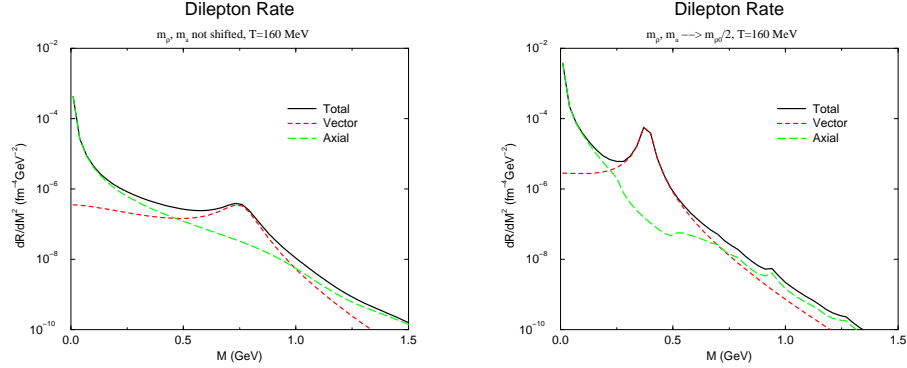


Figure 1: Dilepton production rates (a) standard (b) comparison with maximally shifted according to variant D discussed in section 5.

use expressions recently derived in [19]: They contain processes in zeroth and first order in the pion density. The expression for the dilepton rate reads

$$\frac{dR}{d^4q} = \frac{\alpha^2}{3\pi^3 q^2} \frac{1}{1 + \exp(q_0/T)} \left[ 3q^2 \text{Im}\Pi_v(q^2) + \int \frac{d^3k n(k_0)}{(2\pi)^3 2k_0 f_\pi^2} \right. \\ \left. [-12q^2 \text{Im}\Pi_v(q^2) + 6(k+q)^2 \text{Im}\Pi_a((k+q)^2) + 6(k-q)^2 \text{Im}\Pi_a((k-q)^2)] \right] \quad (3)$$

where  $k$  is the pion and  $q$  is the virtual photon momentum. Here  $\text{Im}\Pi_v, \text{Im}\Pi_a$  are imaginary parts (or spectral densities) for vector and axial currents. If this expression is understood as expansion in the pion density, they should be evaluated in *vacuum*, and thus related to experimental data on  $e^+e^- \rightarrow \text{hadrons}$  and  $\tau$  lepton decay. Furthermore,  $\text{Im}\Pi_v, \text{Im}\Pi_a$  can be approximated by well-known contributions of  $\rho, a_1$  resonances, which produce dileptons by their decays into  $e^+e^-$  and  $\pi e^+e^-$ , respectively. We chose the follow-

ing parametrizations for  $Im\Pi_v$  and  $Im\Pi_a$  (see section 5)

$$Im\Pi_v = \frac{2f_\pi^2}{M^2} \frac{m_{\rho 0}^2 m_\rho \Gamma_\rho}{(M^2 - m_\rho^2)^2 + m_\rho^2 \Gamma_\rho^2} \quad (4)$$

$$Im\Pi_a = \frac{f_a^2 m_a \Gamma_a}{(M^2 - m_a^2)^2 + m_a^2 \Gamma_a^2} \quad (5)$$

where  $f_\pi = 93$  MeV,  $\Gamma_\rho = \Gamma_{\rho 0} \frac{M^2}{m_{\rho 0}^2}$ ,  $\Gamma_{\rho 0} = 149$  MeV,  $m_{\rho 0} = 770$  MeV,  $f_a = 190$  MeV,  $\Gamma_a = \Gamma_{a 0} \frac{M^2}{m_{a 0}^2}$ ,  $\Gamma_{a 0} = 400$  MeV,  $m_{a 0} = 1210$  MeV [19].

The resulting rates [19] are shown in Fig.1(a), where we show the contributions of the vector and axial parts separately. We have used simple Breit-Wigner parametrization<sup>7</sup> with *vacuum* parameters for resonances taken from Particle Data Tables, while part (b) corresponds to both  $\rho, a_1$  masses shifted to  $\frac{1}{2}m_{\rho 0}$  in the “mixed phase”. (We assume the critical temperature  $T_c = 160$  MeV, and the mass shifts will be discussed in detail below). In both cases, the direct channel resonance  $\rho$  dominates around its mass, while the  $a_1$  contribution takes over at small masses.

### 3 The model for the space-time evolution

The hydrodynamical model was suggested by Landau more than 40 years ago, and its applications to heavy ion collisions has a long history. Experiments with heavy ions at lower energies ( $\sim 1$  GeV/A) were able to detect collective motion of nuclear matter by comparing velocity distribution of different nuclear fragments.

One important finding is that in the AGS/SPS energy range for heaviest nuclei (Au Au at AGS and Pb Pb at SPS) the rapidity spectra of  $\pi, K, p, d$

---

<sup>7</sup> This is why vector contributions does not vanish below  $2m_\pi$ .

are consistent [1] with a simple hydro description: a convolution of *thermal motion* at breakup (which depends on the particle mass) with a collective flow *common for all species including baryons*<sup>8</sup>. An open question however is whether thermalization is rapid enough, so that one can use hydro description from very early times, or collective motion is formed only at later stages. In this work we assume that the former is the case, and will use hydro description for dilepton/photon production.

The second important observation is related with the equation of state (EOS). For finite T and *zero* baryon density, a conventional parametrization of the EOS can be given by a “resonance gas” [20] below  $T_c$ , plus a bag-model QGP above  $T_c$ . We fixed the phase transition point (smoothened for numerical purposes) at  $T_c = 160$  MeV. In hadronic phase the speed of sound  $dp/d\epsilon = c_s^2 = 0.19$ , and in the plasma phase the bag constant is  $B = 0.32$  GeV/fm<sup>3</sup>. The results are plotted in Fig.2. This EOS is in reasonable agreement with the lattice results. Unfortunately, there is so far little progress in lattice simulations for non-zero baryon density. People have extrapolated various models which are successful at nuclear densities, like Walecka model, but it is unclear how well such extrapolation works. Some guidance can probably be provided by hadronic gas including baryonic resonances, for example the one discussed in [1]. In Fig.2 we have shown the corresponding curve (dashed line) for baryon chemical potential  $\mu_b = .54$  GeV, corresponding to AGS breakup conditions. In this case the baryon/meson ratio is about 1, one order of magnitude larger than baryon admixture in central region at SPS energies: and still the EOS in  $p, \epsilon$  coordinates looks approximately the same as the one we adopted.

In summary, the first observation shows that for heavy ions the flow of the entropy (mesons) and the baryonic charge (nucleons) are about the same. The second shows that EOS (in  $p(\epsilon)$  form) is not much affected by baryonic charge. Taken together, they provide a reason to *ignore* baryonic charge in our hydro calculations.

---

<sup>8</sup>In the framework of cascade models such as RQMD this topic was studied [21] and it was also concluded that if one cut the excited system into elements, the mean velocity of different species are the same with accuracy 10-20 percent.



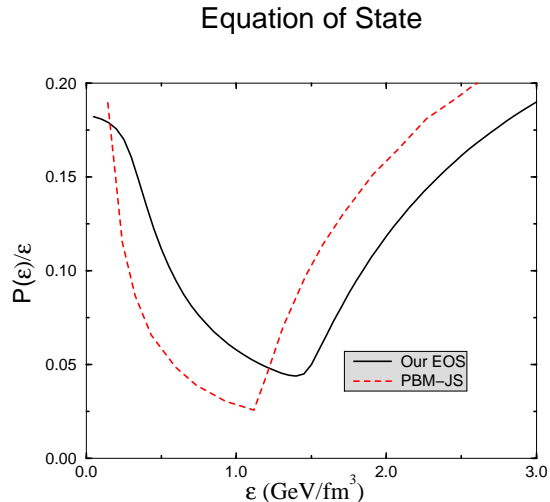


Figure 2: The EOS in hydro-relevant coordinates: the ratio of pressure to the energy density  $p/\epsilon$  versus  $\epsilon$ . Notice the minimum, which we refer to as the “softest point”. The dashed line is the EOS for finite baryon chemical potential  $\mu_b = .54$  GeV from Braun-Munzinger and Stachel.

We use standard equations of (non-viscous) relativistic hydrodynamics for central collisions (i.e. we assume axial symmetry). The hydro equations were solved numerically using the first-order Lax finite difference scheme. Energy and entropy conservation is monitored, and we have also made comparison with results of several earlier works was made to ensure that technical aspects are under control.

The major uncertainties one faces dealing with hydrodynamical models are the initial conditions<sup>9</sup>. Those can be described by the following set of parameters: (i) the initial size  $z_0$ ; (ii) the fraction of thermalized energy/collision energy  $\kappa$ ; and (iii)  $v_{i,z}$  describing initial distribution of the

---

<sup>9</sup> Although cascade-type event generators (Venus, RQMD or ARC) provide some guidance, their physical basis is questionable exactly at the first 1-2 fm/c of the collision, when we need it.

longitudinal velocity

$$v_z(t=0) = v_{i,z} * \tanh(z/z_0) \quad (6)$$

We consider specifically two cases of *central* collisions: (i) S-Au 200 GeV/N and (ii) Pb Au 160 GeV/N for which the dilepton/photon data were taken. In all cases considered, at  $t = 0$  we assume that *some part*  $\kappa$  of total energy goes into the thermalized matter at rest, and fix  $\kappa$  demanding that at the end of the expansion (at  $T_f = 140\text{MeV}$ ) the predicted number of pions<sup>10</sup> is the same as observed.

One extreme scenario is complete equilibration,  $v_{i,z} = 0$  à la Fermi-Landau. Furthermore, if thermalization is very rapid, the usual Lorentz contraction is enhanced by the ordinary compression of matter by shocks, leading to very high  $\epsilon_i \sim 10\text{ GeV/fm}^3$  initial energy density, well above the phase transition region. As shown e.g. in [23] this scenario is incompatible with SPS data on rapidity distribution. However, as shown in Fig.3(a), for  $v_{i,z} = 0.9$  one obtains reasonable description of the longitudinal motion<sup>11</sup>.

## 4 Conventional dilepton yields

Now we evaluate the dilepton yield, by integrating the production rate over the space-time. The integral is taken between the surface at which initial conditions are set (the so called “pre-equilibrium” contribution is thus left over) and the “breakup” surface, at which the density is so small that secondaries

---

<sup>10</sup> Multiple studies have shown that about 1/3 of pions come from resonance decays. We included this fact in the normalization.

<sup>11</sup> Distribution of other secondaries, as well as the *transverse* motion we plan to present elsewhere. The hardon rapidity data is taken from [24] (The data actually refers to negative hadrons. We scaled them by 0.7 to account for resonance decays. The  $y > 2.65$   $\frac{dN}{dy}$  data for S+Au has been reflected about  $y = 2.65$  to give data for  $y < 2.65$ .)

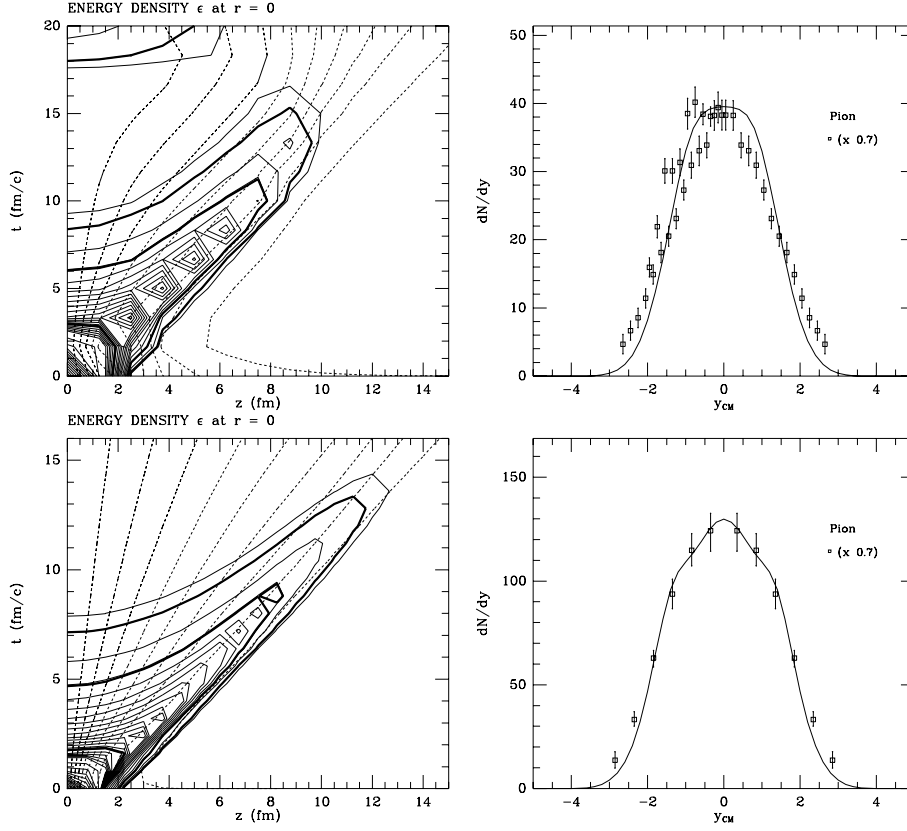


Figure 3: Typical hydro evolutions for 200A GeV S+Au (upper part) and 160A GeV Pb+Au (lower part). The *left* part shows hydrodynamical solution in the plane time-longitudinal coordinate. Solid lines are lines of constant energy density, the dotted ones correspond to constant longitudinal velocity. Thicker lines show the end of the mixed phase ( $\epsilon = 1.47 \text{ GeV/fm}^3$ ) and the break-up conditions ( $\epsilon = 0.31 \text{ GeV/fm}^3$ ): at  $z = 0$  that happens at about time 5 and 7 fm/c, respectively. The figures on the right shows the calculated pion rapidity spectra (lines) compared with data, where the data has been scaled by 0.7 to account approximately for resonances.

can fly away without interaction<sup>12</sup>. The surface should be determined from

<sup>12</sup>In principle, some pion annihilation can happen even later: we have evaluated this contribution and have found that it is small. Note also that  $\rho, \omega, \eta$  etc decays after breakup

the mean free path, and for pions it corresponds to  $T_{breakup} = 140 MeV$ . Furthermore, in order to compare with CERES data one has to apply their experimental cuts: For S+Au,  $p_T > 200 MeV/c$ ;  $\Theta_{ee} > 35 mrad$ ;  $2.1 < \eta < 2.65$ . For Pb+Au,  $p_T > 175 MeV/c$ ;  $\Theta_{ee} > 35 mrad$ ;  $2.1 < \eta < 2.65$ .

The results we obtained are shown in Fig.4(a): they are split into 4 contributions: from pure QGP phase (denoted by Q); QGP part of the mixed phase (Mix/Q); hadronic part of the mixed phase (Mix/H); and finally from the hadronic phase (H). Note that, as expected, QGP contribution dominates at high masses, while hadronic contribution dominates at  $\rho$  region and below. Although in the rates shown in Fig. 1 one can see quite substantial contributions at low masses from  $a_1$  decay, it is reduced by the small experimental acceptance in this region so dramatically that it falls well below the data.

For check of consistency, we have compared our results with those of other approaches in Fig.4(b). All three use “conventional rates” which are similar to ours (except the  $a_1$  part) but very different dynamics of the evolution. Li-Ko-Brown approach is based on cascades started from RQMD-based initial conditions<sup>13</sup>. Srivastava *et.al.* assumed Bjorken-scaling longitudinal hydrodynamics, with solved hydro in the transverse plane<sup>14</sup>. We conclude that the agreement between 3 papers is reasonable in terms of the total yield, and even very good in terms of the shape of the mass spectrum. Since all three results disagree with data, one may conclude that it is not possible to explain CERES data by “conventional sources”.

In Fig.4(c) we also show our predictions for 160A GeV Pb+Au collisions. We compare them with new *preliminary* CERES data reported at Quark Matter 96 [6]. Since the data are for non-central collisions, we have multiplied our curve by the factor 1.7, the ratio of the *observed* dilepton yield for minimum bias sample  $\langle n_{ch} \rangle = 260$  to that in central sample  $\langle n_{ch} \rangle \approx 400$ .

---

are precisely the “hadronic background”, which was separately calculated, by the experimental group itself.

<sup>13</sup>Note that it includes additionally the  $\phi$  contribution ignored by us and others.

<sup>14</sup>Note that this curve is already corrected for the double counting which was present in the original paper, but their results are still somewhat larger.

In this case the disagreement is not statistically as significant as in the previous reaction, but still it seems that the measured shape of the spectrum is different from the predicted one.

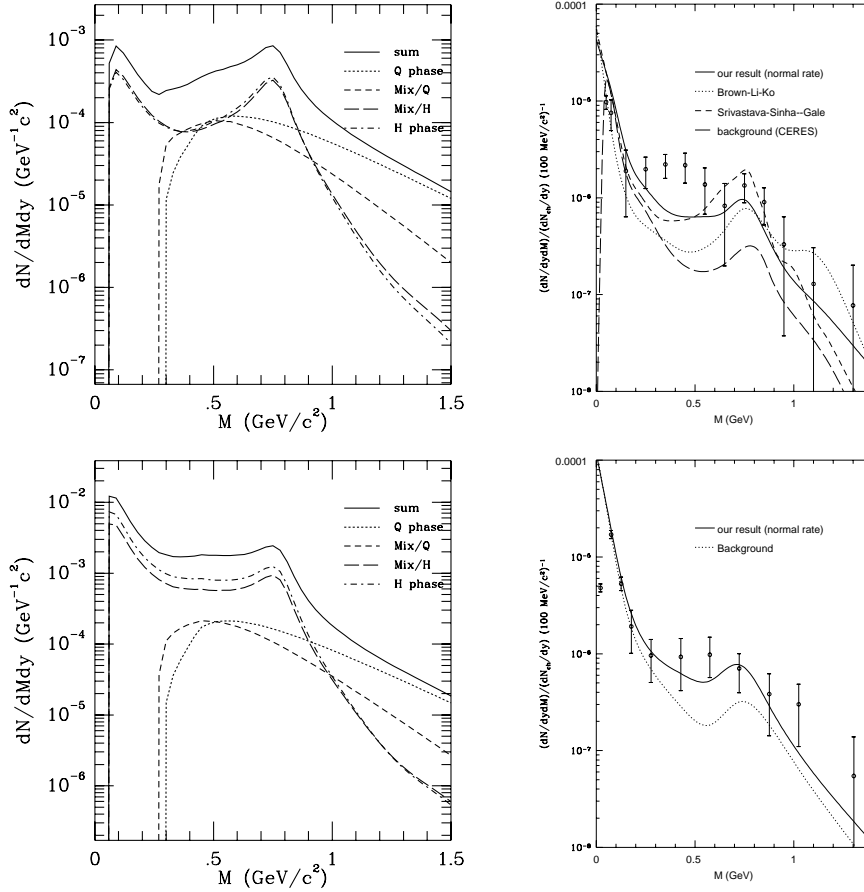


Figure 4: CERES dilepton spectra from conventional sources. (Top) our conventional spectra for 200A GeV S+Au, shown without and with background from hadronic decays; (Bottom) our results for 160A GeV Pb+Au w/o and with background.

## 5 Dilepton yield from modified $\rho, a_1$ mesons

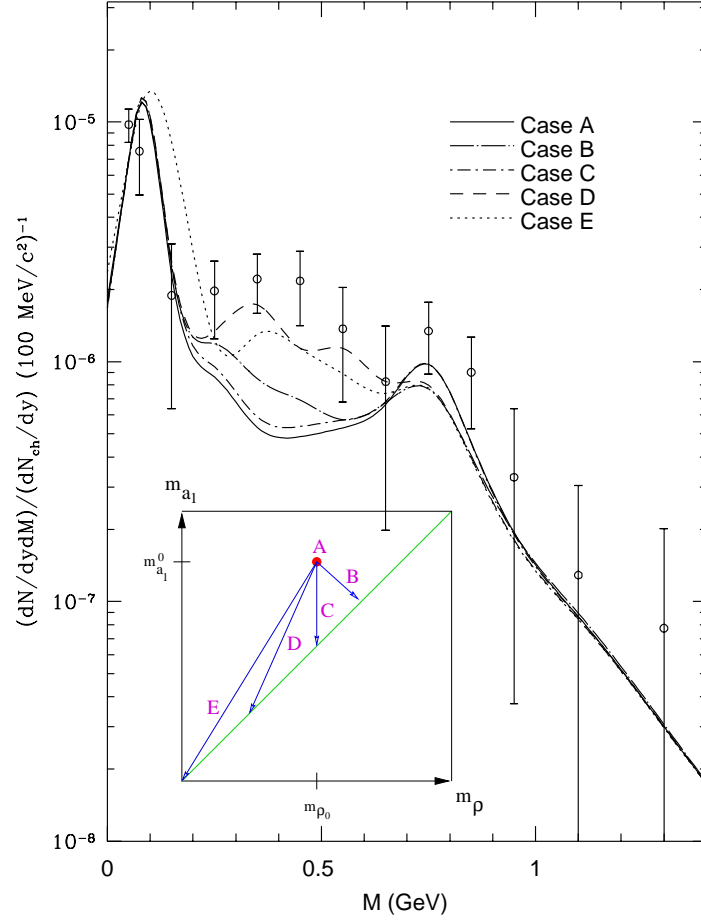


Figure 5: Dilepton yield in 200A GeV S+Au collision for different possible scenario of chiral restoration in  $m_\rho - m_{a_1}$  plane.

Dileptons, unlike secondary hadrons, are produced at relatively early stages of the collisions. One possible explanation of why the “standard” rates fail to reproduce the observed excess of low-mass dileptons may be a long-debated idea: hadronic properties may be *modified* in high density hadronic matter.

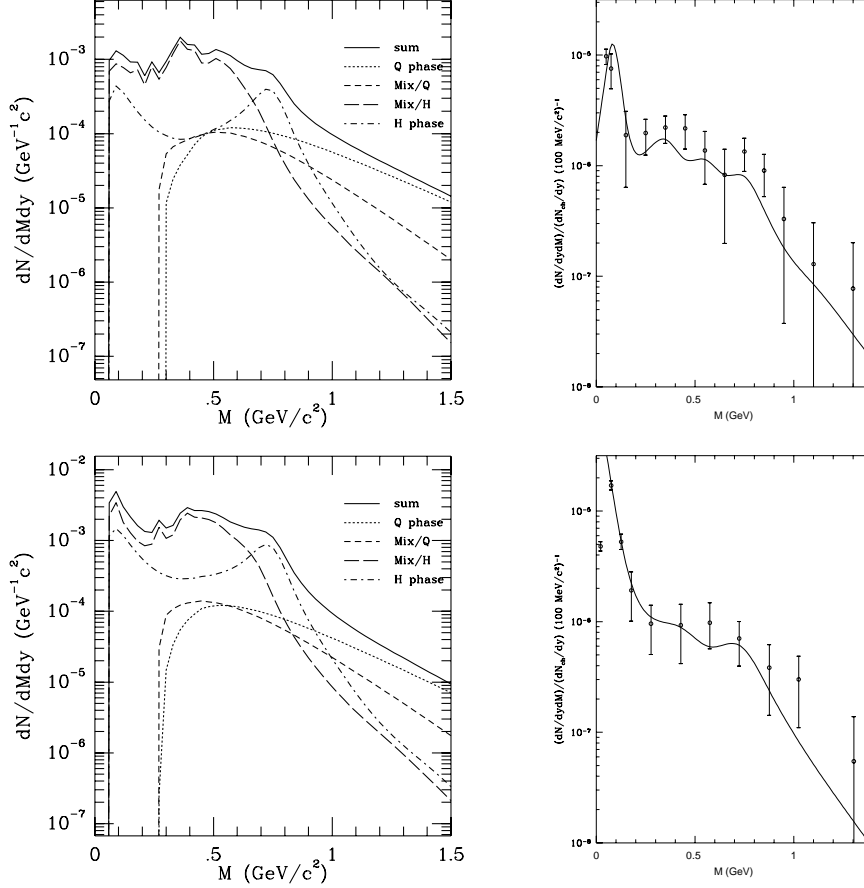


Figure 6: Direct dilepton yields (without and with background) for 200A GeV S+Au (top) and 160A GeV Pb+Au (bottom) using mass scheme D.

We know definitely that the *nucleon* mass is modified in nuclear matter, and shifts of the *vector meson masses* in it are debated for a long time, see e.g. [25, 26].

In a low-T hadronic gas (which may include an admixture of baryons) one can relate modification of mesons (e.g. of  $\rho$ ) to the  $\pi\rho$  (and  $N\rho$ ) for-

ward scattering amplitudes [27]. This approach predicts certain momentum-dependent optical potential, which can be loosely interpreted as (relatively modest) shift of  $m_\rho$  downward. Finite T/density QCD sum rules (see e.g.[28] and references therein) relate hadronic properties to the quark condensate  $\langle \bar{q}q \rangle$ , which decreases toward chiral restoration transition. This reasoning has culminated in the so called *Brown-Rho scaling idea*, according to which all hadronic dimensional quantities get their scale from  $\langle \bar{q}q \rangle$ : therefore *all* masses are predicted to vanish at  $T \rightarrow T_c$ .

In the *instanton model* the chiral restoration is due to transition from random instanton liquid to a gas of instanton-anti-instanton molecules[29]: the latter survive the phase transition and lead to new type of quark interactions unrelated to  $\langle \bar{q}q \rangle$ . Although results of available simulations [30] have not reported any definite conclusions about the rho meson mass, at quark level it was clearly demonstrated that at  $T > T_c$  an effective quark mass is substituted by “effective energy” (or “chiral mass”) of comparable magnitude, which imply that hadronic masses should *not* vanish at  $T \rightarrow T_c$ .

The matter however is by no means settled, and quite different suggestions about hadronic properties close to (or even above)  $T_c$  can be found in literature. For example, effective Lagrangians lead to a prediction of *rising*  $m_\rho(T)$  [31], moving it about half way toward the mass of its chiral partner  $a_1$ . Furthermore, at SPS about 1/10 of secondaries are baryons, and thus finite baryon density effects should be added to the finite-T shifts mentioned above.

Therefore, we have decided to proceed empirically, *assuming* various scenarios of hadronic mass evolution in dense matter. A particular point we want to make in this paper is that “dropping  $m_\rho(T)$ ” idea is consistent with chiral symmetry restoration only if appropriate modifications of its axial partner  $m_{a_1}$  follow. Strict theoretical relation between the two were derived via Weinberg-type sum rules [32]. Possible scenarios of how chiral restoration may proceed are therefore shown in the  $m_\rho - m_{a_1}$  plane in Fig.5(a). For example, path B corresponds to results of Pisarski [31], while E corresponds to Brown-Rho scaling. Anyway, both mesons should become iden-



tical at  $T_c$ , so the path of thermal evolution should end up at the diagonal  $m_\rho(T_c) = m_{a_1}(T_c)$ .

To test these ideas, we need a simple consistent model of *how* a changing  $\rho$  mass can change the dilepton production rates discussed in section 2. In this respect, the standard expression for the pion form-factor (2) happen to be quite misleading: it includes  $m_\rho$  both in numerator and in denominator, but simply to make it T-dependent *everywhere* would in fact be a mistake. Recall the usual reasoning why there is  $m_\rho^4$  in numerator is that at  $M = 0$  the form-factor should be  $F(0)=1$ . This statement should hold for the  $\rho$  contribution only if one assumes the so called *vector dominance*, demanding that the whole form-factor (and not just a part of it) is given by the rho pole. It is quite accurately satisfied at  $T=0$ , but for T-dependent  $m_\rho$  vector dominance has no reason to persist!

Actually the numerator of the form-factor contains a combination  $m_\rho^2 \Gamma_{e^+e^-} \Gamma_\rho$ , and in what follows we assume that both widths are *T-independent*. Note that only assumption  $\Gamma_{e^+e^-} = \text{const}(T)$  is actually important, because (i)  $m_\rho^2$  cancels when one returns to non-relativistic form of Breit-Wigner; and (ii) as we have argued above, the value of the  $\Gamma_\rho$  is nearly irrelevant for the rate anyway.

Let us concentrate only on the  $\rho$  part of the rate and write the dilepton production rate as (see appendix):

$$\begin{aligned} \frac{dR}{d^4k} = & \frac{-\alpha^2}{\pi^3} \frac{m_{\rho_0}^4}{f_\rho^2 M^2} \left(1 + \frac{2m_l^2}{M^2}\right) \left(1 - \frac{4m_l^2}{M^2}\right)^{\frac{1}{2}} \\ & \times \frac{Im\Pi}{\left(M^2 - \hat{m}_\rho^2\right)^2 + (Im\Pi)^2} \left(\frac{1}{e^{\beta\omega} - 1}\right) \end{aligned} \quad (7)$$

where  $\hat{m}_\rho^2 = m_{\rho_0}^2 + Re\Pi$  and  $\Pi$  is the  $\rho$  self-energy. One can define the  $M$ -dependent width of  $\rho$  by the relation  $Im\Pi(T=0) \stackrel{\text{def}}{=} -m_{\rho_0}\Gamma(M)$  which

is generalized to non-zero  $T$  by  $Im\Pi(T, M) = -m_\rho(T, M)\Gamma(M)$  where we ignored the modification of the width with  $T$ . Finally we can rewrite Eq. (7) as

$$\begin{aligned} \frac{dR}{d^4k} = & \frac{2\alpha^2}{\pi^3} f_\pi^2 \frac{m_{\rho_0}^2}{M^2} \left(1 + \frac{2m_l^2}{M^2}\right) \left(1 - \frac{4m_l^2}{M^2}\right)^{\frac{1}{2}} \\ & \times \frac{m_\rho(T)\Gamma(M)}{\left(M^2 - \hat{m}_\rho^2\right)^2 + m_\rho^2(T)\Gamma^2(M)} \left(\frac{1}{e^{\beta\omega} - 1}\right) \end{aligned} \quad (8)$$

where we have suppressed the  $M$ -dependence of  $m_\rho$ ,  $\hat{m}_\rho$  and we used the relation  $f_\pi^2 = \frac{m_{\rho_0}^2}{2f_\rho^2}$ .

For simplicity we identify  $\hat{m}_\rho(t)$  and  $m_\rho(T)$ , with both given by

$$\frac{m(T)}{m_0} = \frac{a}{T/T_c - b} + r - \frac{a}{1 - b} \quad (9)$$

where  $r$  is the value of  $\frac{m(t)}{m_0}$  when  $T = T_c$ ,  $a$  characterizes the abruptness of the mass shift, while  $b$  is chosen to make  $\frac{m(T)}{m_0} = 1$  at  $T = T_f = 140$  MeV.

Now we can test whether a  $T$ -dependent masses can indeed describe the CERES data in the lower mass region. Integrating over space-time according to hydro calculations described above we get the dilepton mass spectra as shown in Fig. 5. The variant D, with  $m_\rho(T_c) = m_{a_1}(T_c) \sim \frac{1}{2}m_\rho(0)$ , does the best job, and Fig.6 we show contribution of separate stages in this scenario, for both 200 A GeV S+Au and 160A GeV Pb+Au. It is the hadronic part of the mixed phase which is responsible for the observed excess at  $M = 0.2 - 0.6$  GeV. Furthermore, depending on how exactly  $m_\rho(T)$  goes to its limit at  $T_c$ , one can change the shape of the resulting mass spectrum. This statement is demonstrated in Fig.7, where (a) shows several scenarios, with the resulting

mass spectra in Fig.7(b). The case E in 5, which corresponds to massless  $\rho$  and  $a_1$ , generates more low-mass pairs than the hadronic cocktail. Better data of  $\eta$  production is needed to rule out this case.

Of course, specific dynamical models lead to more complicated picture: instead of simple universal  $m_\rho(T)$  for any  $\rho$  meson, they lead to specific modification of the whole dispersion curve. Clearly, mesons which travel fast relative to matter are modified differently from those which have zero velocity. Furthermore, since the meson-meson and meson-baryon scattering is dominated by resonances, this dependence may even be non-monotonous. Future high-statistics studies may look into those matters by considering mass spectrum at different rapidity and/or  $p_t$  of the dileptons.

In conclusion: we have demonstrated that the CERES data can be fitted pretty well over the whole experimental mass range by assuming a particular  $m_\rho(T)$ , *without* any change in the production mechanism or space-time evolution.

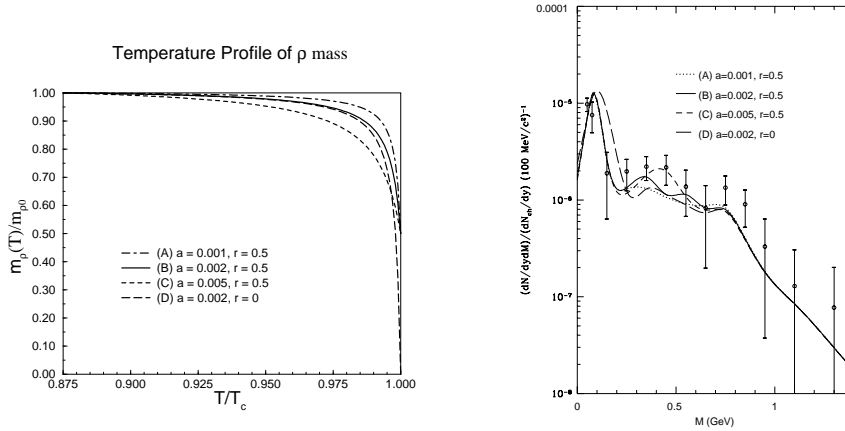


Figure 7: Different temperature profiles for  $m_\rho(T)$  (left) The corresponding dilepton spectra. (right) For meaning of the parameters  $a$  and  $r$ , refer to equation (9)

## 6 Searching for the modified $a_1$ contribution

Great interest related with modified hadronic masses is explained by a possible relation between this phenomenon and the chiral phase transition. As it was repeatedly emphasized above, modification of  $\rho$  imply certain modifications of  $a_1$  as well. In this section we discuss how this can be experimentally verified as well.

The important role of  $a_1$  for production of photons and dileptons was discussed in [16, 5, 17, 18] As we have shown in section 2, the main  $a_1$  contribution is at low dilepton masses. However, CERES has adopted cuts which makes its acceptance very small at small  $M_{e^+e^-}$ , and therefore, the  $a_1$  contribution to its mass spectrum is not very significant. Those cuts were made in order to get rid of hadronic background, such as  $\eta$  Dalitz decay. So, by simply looking at small mass region one cannot find the  $a_1$  contribution.

Nevertheless, one can try to locate a kinematical “window” in which it may be better seen. We have found that the best range of invariant dilepton masses is  $M_{e^+e^-} \approx 300 MeV$ . Above it hadronic background is relatively small, but the contribution of  $\rho$  channel and even of the quark annihilation in the QGP phase exceed the  $a_1$  contribution. Below this mass they are not so important, but soon the hadronic background from ordinary Dalitz decays take over.

Furthermore, there is a particular  $p_t$  dependence of the effect. Consider first the *unmodified*  $a_1$ , decaying into  $\pi e^+ e^-$ . For relatively small dilepton masses, in the  $a_1$  rest frame both the pion and dilepton get half of its total mass. Including thermal motion and (rather large)  $a_1$  width, one still finds a broad maximum in dilepton production rate at dilepton energy about 600 MeV. Integrated over longitudinal momentum, one gets dilepton  $p_t$  distribution shown in Fig.8(a), with a maximum. It looks very different compared to the dileptons coming from  $\rho$  decay and having the usual thermal  $p_t$  dependence. Now comes the main point: *if* the  $a_1$  mass shifts down, as expected from chiral restoration, then the wide peak is absent and the shape is differ-

ent: see Fig.8(b).

In summary, it is important to locate and to test properties of  $a_1$  contribution. We have shown how sensitive dilepton production is to its modification in dense matter. Although this task is not easy, next generation of experiments (with accurate knowledge of hadronic backgrounds, measured dependence on the event centralities etc) can in principle do it.

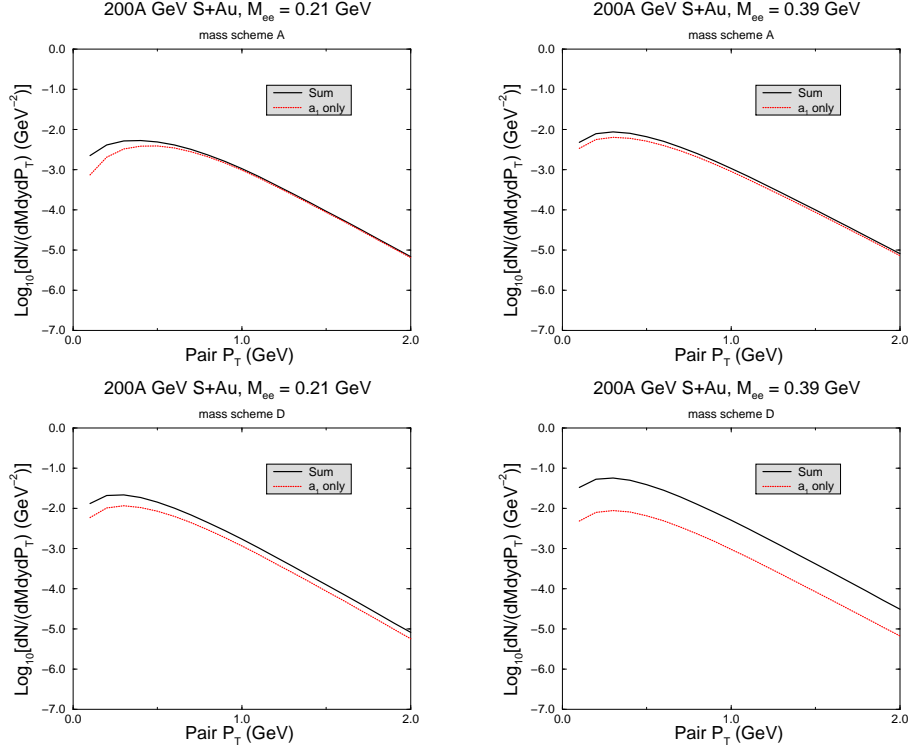


Figure 8: Dilepton  $p_t$  spectrum for 200A GeV S+Au. The top two figures are for mass scheme A (i.e. unshifted masses) while the bottom two are for mass scheme D.

## 7 Can one explain the dilepton excess by a long-lived fireball?

In our previous work [14] it was shown, that under certain conditions the “softness” of EOS near the phase transition can affect the *longitudinal* expansion, so that even the global lifetime of the excited system increases substantially. It happens in a *window* of collision energies such that the initial energy density is close to the “softest point”, which makes secondary acceleration of matter impossible. Due to uncertain initial conditions, we do not exactly know to which collision energies this window correspond, but estimates put it in the region  $E_{LAB} \sim 30 \text{ GeV}/A$ , between AGS and SPS. Some examples of the solution we got at higher energies and at the softest point are shown in Fig.9. One can see that the long-lived fireball is slowly burning, with the lifetime reaching more than 30 fm/c!

It was further been proposed that one can test these unusual predictions experimentally by: (i) Looking for the maximal lifetime (or the minimum of the HBT parameter  $\lambda$ ) [14]; (ii) Looking for the *minimum* of the “directed” flow in the collision plane [33]; (iii) Looking for the nearly isotropic distribution of dileptons, produced in the long-lived fireball [14]. In connection with (i) it is very intriguing that the E802 AGS experiment reported preliminary studies of HBT which indicate significant ( $\sim 40\%$ ) growth of lifetime for the most central Au Au collisions [34].

We now would like to check whether the long-lived fireball, *if present at SPS energies*, can enhance the dilepton production to a degree necessary to explain the CERES data. For that we take the initial conditions as shown in Table 1, which indeed give the initial energy density close to the softest point value.

The results however indicate that this scenario can neither be made consistent with rapidity distribution of secondaries, nor does it actually result in larger production of dileptons. In Fig.10 we compare two expansion scenarios with *unmodified* masses. The reason for this is as follows: longer lifetime is

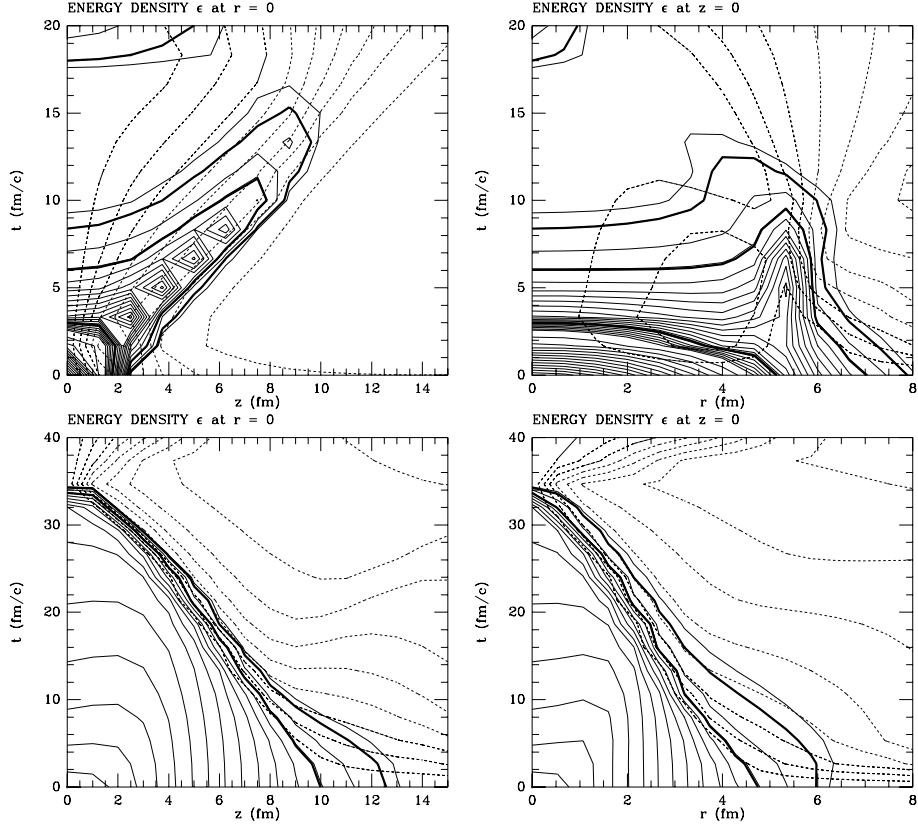


Figure 9: Space-time evolutions for Standard Bjorken-like scenario (top)  
Long-lived fireball scenario (bottom)

compensated by smaller 3-volume. And also, the shape of the dilepton mass spectrum is different from the observed one.

Furthermore, if masses are modified (say according to variant D of Fig.5(a)), both space-time pictures become compatible with data, see Fig.11.

Table 1: Parameters for the two hydro models used

	Bjorken-like	Long-lived Fireball
Initial energy density $\epsilon_i(\text{GeV}/\text{fm}^3)$	9.0	1.5
Initial temperature $T_i(\text{GeV})$	0.27	0.16
Total energy in fireball $E_i(\text{GeV})$	830	930
Initial long. velocity $v_{z0}/c$	0.0	0.0
Initial transverse vel. $v_{r0}/c$	0.0	0.0
Initial long. half-size $z_0(\text{fm})$	1.1	8.0
Initial transverse radius $r_0(\text{fm})$	3.8	3.8
Critical temperature $T_c(\text{GeV})$	0.16	0.16
Freeze-out temperature $T_f(\text{GeV})$	0.14	0.14

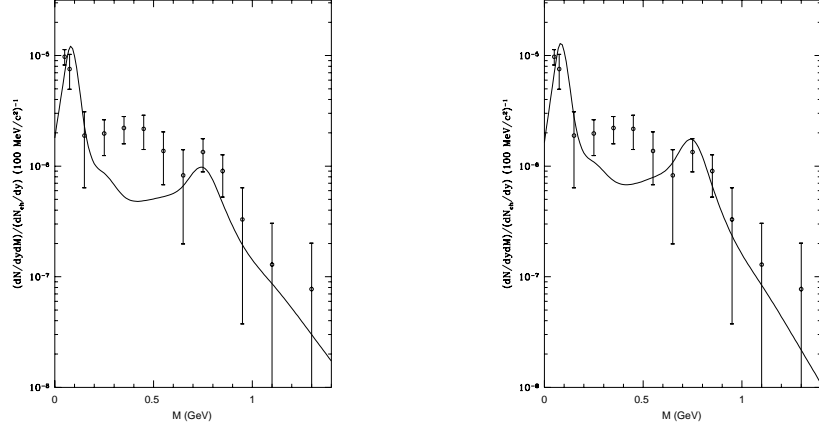


Figure 10: 200A GeV S+Au direct dilepton yields using unshifted masses for the usual Bjorken-like expansion (left), and for the long-lived fireball (right)

## 8 Photon production

Let us briefly comment on the history of theoretical and experimental studies for photon production. As for dileptons, the radiation from QGP phase was already calculated in [2]. Reactions in a gas of  $\pi, \rho$  mesons were considered in



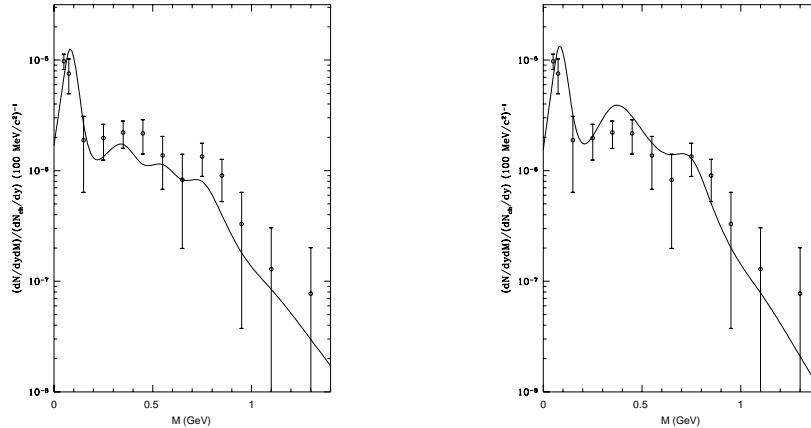


Figure 11: 200A GeV S+Au direct dilepton mass spectrum using the  $\rho$ ,  $a_1$  masses in scenario D for Bjorken-like hydro (left) and for the long-lived fireball (right)

[15], and importance of  $a_1 \rightarrow \gamma\pi$  reactions was pointed out in [16]. Following our dilepton calculations, we use the photon rate given in [19].

Experimental observation of direct photons is an extremely difficult task. Unlike dileptons, we cannot tune the invariant mass and therefore for all photon momenta the background from hadronic decays (mostly  $\pi^0$ ,  $\eta$ ) dominates the signal of the “direct” photons. Therefore, the issue is very accurate measurements of these backgrounds and inclusive photon spectra, with subsequent subtraction. At the moment, only upper bounds on the direct photon cross section has been given by the WA80 experiment [35]<sup>15</sup>.

---

<sup>15</sup> Earlier preliminary WA80 data indicated a non-zero effect: its comparison with theoretical expectations based on “standard sources” [5] lead to conclusion that those data significantly exceeded the expectations. Later in [22] this conclusion was disputed: larger photon yield (now consistent with data) was obtained. The issue under debate was basically how one should normalize the hydrodynamical initial conditions. Eventually, the *preliminary* data were withdrawn after the reanalysis.

In Fig.12 we show results of our calculations of the direct photon production. They correspond to unmodified hadronic parameters, and are performed both for standard space-time scenario (a) and the long-lived fireball (b). The main conclusions are: (i) The theoretical predictions are in both cases *below* the experimental bound in the whole region, although the difference between them is not that large. (ii) The two scenarios show significant difference at large  $p_t \sim 3\text{GeV}$ , mostly due to existence of relatively hot QGP in the first case. It would be very important to pursue the issue further, in WA80 or elsewhere, and try to observe radiation from QGP and hot hadronic gas.

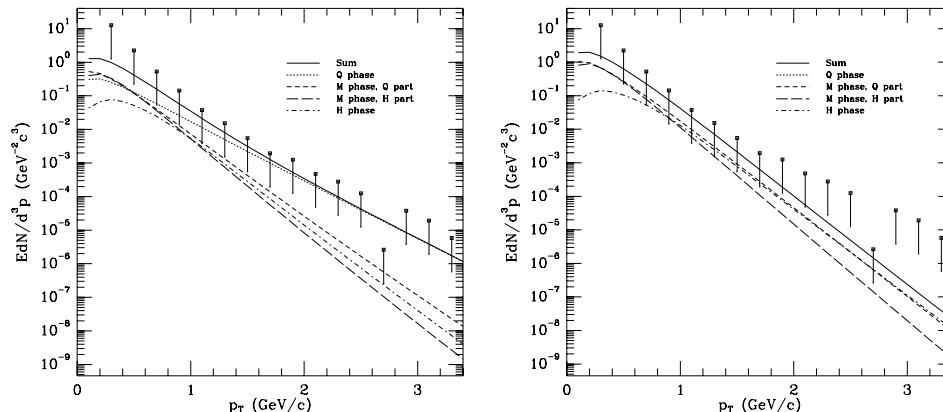


Figure 12: Direct photon production in 200A GeV S+Au compared with preliminary WA80 upper bounds on direct photon production. Our predictions are for the Bjorken-like expansion (left) with hot initial stage, and for the long-lived fireball. (right)

## 9 Conclusions

In summary, we have studied dilepton/photon production from highly excited hadronic matter produced in heavy ion collisions.

Using the rates from the usual hadronic reactions with *vacuum* parameters and the usual hydro description of space-time picture, we obtained results which are consistent with those of previous works but cannot account for low-mass dilepton excess observed by CERES experiment. However, if the  $\rho$  mass is shifted to about 1/2 of its value around the critical temperature, the data can be explained. More detailed observed distribution (e.g. over dilepton mass and  $p_t$ ) should provide better understanding of whether this explanation of the observed dilepton excess is in fact correct.

Furthermore, we have pointed out that chiral restoration demands that the mass of  $a_1$  meson should be shifted together with the mass of  $\rho$ . In order to get more convincing evidence that the excited matter is indeed approaching chiral restoration, experimental observation of the  $a_1$ -related component is essential. We discussed in which kinematical window one should look for it, and evaluated the magnitude of the effect.

Among suggestions to explain the dilepton excess was a proposal that the space-time picture of heavy ion collisions can in fact be different, with possibly a longer-lived fireball. However, although for specific initial conditions this long-lived scenario is hydrodynamically possible, it does *not* significantly enhance production of dileptons because longer lifetime is compensated by smaller spatial volume. Furthermore, this scenario is incompatible with the observed spectra of secondaries.

Finally, all scenarios considered lead to *photon* production well below current upper limit on direct photons from WA80. The results however are sensitive to expansion scenario. The QGP component in particular becomes dominant around  $p_t \sim 3\text{GeV}$ .

**Acknowledgments** We'd like to thank G.Brown, I.Zahed, M.Prakash and J.Steele for stimulating discussions. This work is supported by the US Department of Energy under Grant No. DE-FG02-88ER40388.

## Appendix: Thermal Dilepton Rate

It can be shown [36] that the thermal rate of dilepton production in a hot hadron gas is:

$$\frac{dR}{d^4k} = \frac{2e^2}{(2\pi)^6} \frac{1}{(k^2)^2} \text{Im}\Pi_{\mu\nu}^R(k) \frac{1}{e^{\beta\omega} - 1} \int \frac{d^3p_+}{E_+} \int \frac{d^3p_-}{E_-} \delta^4(p_+ + p_- - k) \left[ p_+^\mu p_-^\nu + p_+^\nu p_-^\mu - g^{\mu\nu}(p_+ \cdot p_- + m_l^2) \right] \quad (10)$$

Using vector dominance to relate the imaginary part of the photon self-energy  $\Pi_{\mu\nu}^R$  and the imaginary part of the  $\rho$  propagator  $\Delta_{\mu\nu}^R$  [36], then integrating over  $p_+$  and  $p_-$ , we get

$$\frac{dR}{d^4k} = \frac{\alpha^2}{3\pi^3} \frac{m_\rho^4}{f_\rho^2 M^4} \left( 1 + \frac{2m_l^2}{M^2} \right) \left( 1 - \frac{4m_l^2}{M^2} \right)^{\frac{1}{2}} (k^\mu k^\nu - M^2 g^{\mu\nu}) \times \text{Im}\Delta_{\mu\nu}^R(k) \frac{1}{e^{\beta\omega} - 1} \quad (11)$$

This can be manipulated further into the form [37][36]

$$\frac{dR}{d^4k} = \frac{2\omega dR}{dM^2 d^3\mathbf{k}} = \frac{-\alpha^2}{\pi^3} \frac{m_\rho^4}{f_\rho^2 M^2} \left( 1 + \frac{2m_l^2}{M^2} \right) \left( 1 - \frac{4m_l^2}{M^2} \right)^{\frac{1}{2}} \times \frac{\text{Im}\Pi}{(M^2 - \hat{m}_\rho^2)^2 + (\text{Im}\Pi)^2} \left( \frac{1}{e^{\beta\omega} - 1} \right) \quad (12)$$

where  $\hat{m}_\rho^2 \equiv m_\rho^2 + \text{Re}\Pi$  and  $\Pi$  is now the transverse or longitudinal part of the  $\rho$  self-energy. We'd now demonstrate that the above rate can be written

in terms of thermal  $\rho$  decay rates. we are interested in the invariant mass distribution (assuming  $\Pi = \Pi(M)$ ),

$$\frac{dR}{dM^2} = \frac{-\alpha^2}{2\pi^3} \frac{m_\rho^4}{f_\rho^2 M^2} \left(1 + \frac{2m_l^2}{M^2}\right) \left(1 - \frac{4m_l^2}{M^2}\right)^{\frac{1}{2}} \frac{Im\Pi}{\left(M^2 - \hat{m}_\rho^2\right)^2 + (Im\Pi)^2} \times \int \frac{d^3\mathbf{k}}{\omega} \frac{1}{e^{\beta\omega} - 1} \quad (13)$$

which in the Boltzmann approximation reduces to:

$$\frac{dR}{dM^2} = \frac{-2\alpha^2}{\pi^2} \frac{m_\rho^4}{f_\rho^2 M^2} M T K_1\left(\frac{M}{T}\right) \left(1 + \frac{2m_l^2}{M^2}\right) \left(1 - \frac{4m_l^2}{M^2}\right)^{\frac{1}{2}} \times \frac{Im\Pi}{\left(M^2 - \hat{m}_\rho^2\right)^2 + (Im\Pi)^2} \quad (14)$$

Following the notations of [38] we write the dilepton rate as:

$$\frac{dR}{dM^2} = \frac{\alpha^2}{24\pi^3} M T K_1\left(\frac{M}{T}\right) \left(1 + \frac{2m_l^2}{M^2}\right) \left(1 - \frac{4m_l^2}{M^2}\right)^{\frac{1}{2}} F_{eff}(M) \quad (15)$$

where we define

$$F_{eff}(M) \equiv \frac{m_\rho^4 \left(-\frac{48\pi}{f_\rho^2 M^2} Im\Pi\right)}{\left(M^2 - \hat{m}_\rho^2\right)^2 + (Im\Pi)^2} \quad (16)$$

To one loop[36] (i.e. consider only  $\pi - \pi$  annihilation), we have

$$Im\Pi = -\frac{f_\rho^2}{48\pi}M^2 \left(1 - \frac{4m_\pi^2}{M^2}\right)^{\frac{3}{2}} \theta(M^2 - 4m_\pi^2) \quad (17)$$

Thus we recover the usual form of the form-factor,

$$F_{eff}(M)(1 \text{ loop}) = \frac{m_\rho^4}{(M^2 - \hat{m}_\rho^2)^2 + (m_\rho \Gamma_{\rho \text{ total}})^2} \left(1 - \frac{4m_\pi^2}{M^2}\right)^{\frac{3}{2}} \times \theta(M^2 - 4m_\pi^2) \quad (18)$$

where we've defined  $Im\Pi \equiv -m_\rho \Gamma_{\rho \text{ total}}$  as usual.

If we include other interactions besides  $\pi - \pi$  annihilation, in general  $Im\Pi$  (or  $\Gamma_{\rho \text{ total}}$ ) will increase, which increases the width of  $F_{eff}$  in Eq. (16). However, the maximum of  $F_{eff}$  is given by

$$F_{eff \text{ max}} = F_{eff}(\hat{m}_\rho) = -\frac{48\pi m_\rho^4}{f_\rho^2 \hat{m}_\rho^2 Im\Pi} \quad (19)$$

where we assumed that  $\hat{m}_\rho$  and  $\frac{Im\Pi}{M^2}$  are slowly varying functions of  $M$ . Thus we see that the peak of  $F_{eff}$  decreases with increasing  $Im\Pi$ . This contradicts the conclusions in [38] where increases in *both* the width and height of  $F_{eff}$  were reported. The discrepancy can partly be explained by double counting of dilepton rates in [39], which is the basis for  $F_{eff}$  in [38]. To see this, we rewrite the dilepton rate (13) as

$$\frac{dR}{dM^2} = \frac{3}{8\pi^4} \frac{m_\rho^2 \Gamma_{\rho \text{ total}}(M) \Gamma_{\rho \rightarrow ll}(M)}{(M^2 - \hat{m}_\rho^2)^2 + (m_\rho \Gamma_{\rho \text{ total}})^2} \int \frac{d^3\mathbf{k}}{\omega} \frac{1}{e^{\beta\omega} - 1} \quad (20)$$

where the decay widths are given by [37]<sup>16</sup>

$$\Gamma_{\rho \rightarrow ll}(M) = \frac{\alpha^2}{f_\rho^2/4\pi} \left( \frac{m_\rho^3}{3M^2} \right) \left( 1 + \frac{2m_l^2}{M^2} \right) \left( 1 - \frac{4m_l^2}{M^2} \right)^{\frac{1}{2}} \quad (21)$$

$$\begin{aligned} \Gamma_{\rho \text{ total}}(M) \simeq \Gamma_{\rho \rightarrow \pi\pi}(M) &= \frac{f_\rho^2}{48\pi} \frac{M^2}{m_\rho} \left( 1 - \frac{4m_\pi^2}{M^2} \right)^{\frac{3}{2}} \theta(M^2 - 4m_\pi^2) \\ &= -\frac{Im\Pi}{m_\rho} \end{aligned} \quad (22)$$

We note that (20) is essentially the same as the thermal  $\rho$  decay rate (2.9) of [39], which was *added* to the  $\pi - \pi$  annihilation and other reactions in [39]. But Eq. (20) is simply a statement of the fact that the dilepton rate can be interpreted *either* as coming from annihilation of pions *or* as coming from the decay of thermal  $\rho$ 's, the invariant mass distribution of which is given by the Breit-Wigner form (see also [40][37]). We cannot, however, include *both* the thermal decay of  $\rho$ 's and  $\pi - \pi$  annihilation. Doing so, as in [39] amounts to double-counting of the dilepton rates coming from the  $\rho$  channel.<sup>17</sup>

---

<sup>16</sup>Note that  $\Gamma_{\rho \rightarrow \pi\pi}$  in (2.18) of [37] has a factor of 16 instead of 48.

<sup>17</sup>In [41] this double-counting has been noted and corrected

## References

- [1] P. Braun-Munzinger and J. Stachel, nucl-th/9606017, June 1996; P. Braun-Munzinger, J. Stachel, J.P. Wessels, N. Xu, Phys. Lett. B365, 1 (1996), Phys. Lett. B344, 43 (1995).
- [2] E.Shuryak Phys.Lett.78B, 150,1978, Sov.J.Nucl.Phys.28, 408,1978.
- [3] E. Shuryak, Phys. Rev. Lett. 68 (1992) 3270-3272.
- [4] K. Geiger, Phys.Rept. 258, 237-376,1995.
- [5] L. Xiong and E. Shuryak, Phys. Let. **B333**(1994)316.
- [6] CERES Collaboration (G. Agakichev et al.) Phys.Rev.Lett.75:1272-1275,1995. Also Thomas Ullrich's talk at Quark matter 96, Heidelberg, June 1996.
- [7] G.Q. Li, C.M. Ko, and G.E. Brown. *Phys. Rev. Lett.*, 75:4007, 1995.
- [8] M.Hofman et al. *Nucl. Phys.*, A556:15c, 1994.
- [9] B. Kaempfer, P. Koch, and O.P. Pavlenko. *Phys. Rev.*, C49:1132, 1994.
- [10] E. V. Shuryak. *Comm. Nucl. Part. Phys.*, 21:235, 1994.
- [11] J. Kapusta, D. Kharzeev, and L. McLerran. *Phys. Rev.*, D53:5028, 1996.
- [12] Xin nian Wang, 1996. Talk at INT/RHIC Seattle workshop, Jan.96.
- [13] Chungsik Song, V. Koch, Su Houng Lee, and C.M.Ko. *Phys. Lett.*, B366:379, 1996.
- [14] C.M. Hung and E. Shuryak. *Phys. Rev. Lett*, 75:4003, 1995.
- [15] J. Kapusta, P. Lichard, and D. Seibert, *Phys. Rev.*, **D44** (1991)2774.
- [16] Li Xiong, E.Shuryak, G.E.Brown, Phys.Rev.D46 (1992) 3798; C.Song, Phys.Rev.C, 47 (1993) 2861.
- [17] Chungsik Song. *Phys. Rev.*, C 47:2861, 1993.



- [18] Chungsik Song, Che Ming Ko, and C. Gale. *Phys. Rev.*, D 50:1827, 1994.
- [19] J.V.Steel, H.Yamagishi, and I.Zahed. Dilepton and Photon emission rates from a hadronic gas, hep-ph/9603290.
- [20] E.Shuryak, Yadernaya Fis. (Sov.J. of Nucl. Phys.) 16 (1972) 395; R. Venugopalan and M. Prakash, Nucl. Phys. **A546** (1992) 718.
- [21] H. Sorge, Phys.Lett.B373:16-22,1996.
- [22] D.K. Srivastava and B. Sinha, Phys.Rev.Lett.73,2421 (1994)
- [23] N. Arbex, U. Ornik, M. Plümer, A. Timmermann and R.M. Weiner, SLAC preprint HEP-PH-9411336
- [24] Peter Seyboth *et.al.*, FIRST RESULTS FROM THE STUDY OF Pb-Pb COLLISIONS AT 158 GEV PER NUCLEON PROJECTILE ENERGY, NA49 preprint, 1995.
- [25] G.E. Brown, M. Rho, M. Soyeur Nucl. Phys. A553 (1993) 705c-708c.
- [26] T. Hatsuda, H. Shiomi, and H. Kuwabara. LIGHT VECTOR MESONS IN NUCLEAR MATTER. UTHEP-331, Mar 1996. 33pp. Submitted to Prog. Theor. Phys. e-Print Archive: nucl-th/9603043.
- [27] E.V. Shuryak, Nucl.Phys.A533:761-788,1991.
- [28] T. Hatsuda and T. Kunihiro. *Phys. Rep.*, 247:221, 1994.
- [29] T. Schäfer, E. V. Shuryak, and J. J. M. Verbaarschot. *Phys. Rev.*, D51:1267, 1995.
- [30] T. Schäfer and E. V. Shuryak. *preprints, Stony Brook, SUNY-NTG-95-22,23* hep-ph/9509337,9512384. Phys.Rev.D, in press.
- [31] R.D.Pisarski. *Phys. Rev.*, D52:3773, 1995.
- [32] J. Kapusta and E. V. Shuryak. *Phys. Rev.*, D49:4694, 1994.
- [33] Dirk H. Rischke and Miklos Gyulassy. *Nucl. Phys.*, A597:701, 1996.

- [34] M.Baker. Intriguing centrality dependence of the Au Au Source size at the AGS, Talk at Snowbird workshop, Feb.1996.
- [35] P.Stankus, 1996. Measuring direct photons..., Talk at INT/RHIC Seattle workshop, Jan.96.
- [36] C. Gale and J.I. Kapusta, Nucl.Phys. **B357**, 65 (1991).
- [37] P. Koch, Z.Phys. **C57**, 283 (1993).
- [38] D.K. Srivastava, J. Pan, V. Emel'yanov, C. Gale, Phys.Lett. **B329**, 157 (1994).
- [39] C. Gale and P. Lichard, Phy.Rev.D **49**, 3338 (1994).
- [40] H.A. Weldon, Ann.Phys. **228**, 43 (1993).
- [41] D.K. Srivastava, R. Sinha and C. Gale, Phys. Rev. C **53**, R567 (1996).